Fluorescent probes for two-photon microscopy

APPLICATIONS IN NEUROSCIENCES AND BEYOND.

Defining characteristics of two-photon excitation

Two-photon excitation (TPE) is a nonlinear optical process first predicted theoretically by Maria Göppert-Mayer in 1931.[1] Its application to fluorescence microscopy was pioneered much more recently by Denk, Strickler, and Webb.[2] In TPE, a fluorophore is excited via near-simultaneous absorption of two photons, each having half the energy (twice the wavelength) required for the transition from the ground to the first singlet excited state (Figure 1). The prerequisite for near-simultaneous absorption and the timescale of molecular light absorption (~10^{-16} seconds) dictates the use of specialized excitation sources; in current instruments, this is typically a mode-locked Ti-Sapphire laser delivering infrared light pulses of femtosecond duration at high repetition rates.[3] Two-photon excited fluorescence has a characteristic dependence on the square of the excitation light intensity—doubling the excitation intensity quadruples the fluorescence signal. In contrast, fluorescence derived from conventional one-photon absorption exhibits linear dependence on excitation light intensity.

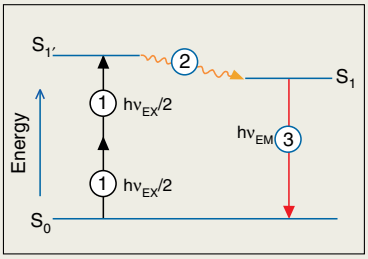

Figure 1—Excited state energy diagram showing two-photon excitation (1) followed by nonradiative vibrational relaxation (2) and spontaneous fluorescence photon emission (3). In conventional fluorescence detection systems, excitation is achieved by absorption of a single photon of energy hu_{EX}; processes (2) and (3) are essentially the same.

There are many practical benefits to using TPE, given the transparency of tissues to infrared excitation light:

- spatial confinement of fluorescence to a very small volume (~0.1 µm^3) defined by the focused excitation light, providing inherent 3D imaging capability (Figure 2)
- capacity for imaging at increased depths in tissues[4]
- confinement of photodamage and photobleaching effects to the excitation volume, resulting in increased viability of living specimens[5,6]

Figure 2—An experiment illustrating ordinary (single-photon) excitation of fluorescence and two-photon excitation. The cuvette contains a solution of the dye safranin O, which normally emits yellow light when excited by green light. The upper lens focuses green (543 nm) light from a CW helium–neon laser into the cuvette, producing the expected conical pattern of excitation (fading to the left). The lower lens focuses pulsed infrared (1,046 nm) light from a neodymium–YLF laser. In two-photon absorption, the excitation is proportional to the square of the intensity; thus, the emission is confined to a small point focus (see arrow), which can be positioned anywhere in the cuvette by moving the illuminating beam. Image contributed by Brad Amos, Science Photo Library, London.

However, in addition to requiring specialized (and therefore fairly expensive) excitation sources, TPE produces photodamage and photobleaching effects within the confined excitation volume that are often more acute than those produced by laser scanning confocal microscopy.[7–10] The advantages of TPE primarily relate to imaging of living specimens. Accordingly, neuroscience—specifically structural and functional imaging of the nervous system—is the largest field of current applications (Table 1). In addition to providing benefits for fluorescence microscopy, TPE offers advantages in other biophotonic techniques such as fluorescence correlation spectroscopy,[11] controlled photoablation,[12] photodynamic therapy,[13] and activation of "caged" compounds.[14] To learn more about the technical foundations and applications of TPE microscopy, researchers should consult the growing collection of available review literature.[15–20]

Table 1—Selected applications of fluorescent probes for two-photon excitation (TPE) microscopy.

Probe	Cat. no.	TPE excitation wavelength	Application	References
Alexa Fluor® 488 phalloidin	A12379	720 nm or 830 nm	Imaging F-actin organization in pancreatic acinar cells	*J Biol Chem* 279:37544–37550 (2004)
Alexa Fluor® 594 hydrazide	A10438, A10442	810 nm	Ca^{2+}-insensitive, neuronal tracer *	*Neuron* 33: 439–452 (2002); www.stke.org/cgi/content/full/sigtrans;2004/219/pl5
Amplex® Red reagent	A12222, A22177	750 nm or 800 nm	Detection of reactive oxygen species (ROS) associated with amyloid plaques	*J Neurosci* 23:2212–2217 (2003)
CFSE, CMTMR	C1157, C2927	820 nm	Tracking T- and B-lymphocyte and dendritic cell motility patterns in intact mouse lymph nodes †	*Science* 296: 1869–1873 (2002); *Proc Natl Acad Sci U S A* 101: 998–1003 (2004)
CM-H_2DCFDA	C6827	740 nm	Detection of localized reactive oxygen species release in cardiomyocytes ‡	*J Biol Chem* 278: 44735–44744 (2003)
DAPI, Hoechst 33342	D1306, D3571, D21490, H1399, H3570, H21492	740 nm	Imaging DNA in nuclei and isolated chromosomes	*Micron* 32:679–684 (2001); *Histochem Cell Biol* 114:337–345 (2000)
DiD	D307, D7757	817 nm	Intravital imaging of mouse erythrocytes	*Proc Natl Acad Sci U S A* 102:16807–16812 (2005)
FM® 1-43	T3163, T35356	840 nm	Monitoring synaptic vesicle recycling in rat brain slices	*Biotechniques* 40:343–349 (2006)
Fluo-5F §	F14221, F14222	810 nm	Imaging Ca^{2+} concentration dynamics in dendrites and dendritic spines	*Neuron* 33:439–452 (2002); www.stke.org/cgi/content/full/sigtrans;2004/219/pl5
Fura-2	F1200, F1201, F1221, F1225, F6799, F14185	780 nm	Detection of GABA-mediated Ca^{2+} transients in rat cerebellar Purkinje neurons	*J Physiol* 536:429–437 (2001)
Lucifer yellow CH	L453, L682, L1177	850 nm	Identification of gap junctions in rat brain slices	*J Neurosci* 23:9254–9262 (2003)
Laurdan	D250	800 nm	Detection of ordered membrane lipid domains	*Proc Natl Acad Sci U S A* 100:15554–15559 (2003); *J Cell Biol* 174:725–734 (2006)
Monochlorobimane	M1381MP	780 nm	Imaging glutathione levels in rat brain slices and intact mouse brain	*J Biol Chem* 281:17420–17431 (2006)
MQAE	E3101	750 nm	Fluorescence lifetime imaging (FLIM) of intracellular Cl^- concentrations in olfactory sensory neurons	*J Neurosci* 24:7931–7938 (2004)
Oregon Green® 488 BAPTA-1	O6806, O6807	880 nm	Imaging spatiotemporal relationships of Ca^{2+} signals among cell populations in rat brain cortex	*Proc Natl Acad Sci U S A* 102:14063–14068 (2005)
Qdot® 525, Qdot® 585, Qdot® 655 nanocrystals	Q11441MP, Q10111MP, Q11621MP, Q11421MP	750 nm	Multiplexed immunohistochemical analysis of arterial walls **	*Am J Physiol* 290:R114–R123 (2006)
SBFI	S1262, S1263, S1264	760 nm	Imaging of intracellular Na^+ gradients in rat cardiomyocytes	*Biophys J* 87:1360–1368 (2004)
TMRE	T669	740 nm	Mitochondrial membrane potential sensor ‡	*J Biol Chem* 278:44735–44744 (2003)
X-rhod-1	X14209, X14210	900 nm	Simultaneous imaging of GFP-PHD translocation and Ca^{2+} dynamics in cerebellar purkinje cells	*J Neurosci* 24:9513–9520 (2004)

* Used in combination with fluo-4, fluo-5F, or fluo-4FF to obtain ratio signals that are insensitive to small changes in resting Ca^{2+} and are independent of subcellular compartment volume. † Multiplexed (single excitation/dual channel emission) combination of CFSE and CMTMR. § Techniques also applicable to fluo-4 and fluo-4FF indicators. ‡ Multiplexed (single excitation/dual channel emission) combination of TMRE and CM-H_2DCFDA. ** Multiplexed (single excitation/dual channel emission) combination of Qdot® 585 and Qdot® 655 nanocrystals. PHD = pleckstrin homology domain.

Fluorescence excitation and emission spectra

One-photon and two-photon excitation of a given fluorophore generally result in identical fluorescence emission spectra, as the originating excited state and the photon emission process are the same (Figure 1). However, two-photon excitation spectra differ from their one-photon counterparts to an extent that depends on the molecular orbital symmetry of the fluorophore (greater difference for higher symmetry fluorophores).[18] Consequently, most two-photon excitation spectra are blue-shifted and broader compared to the corresponding one-photon spectra plotted on a doubled wavelength axis. Simply stated, a fluorophore with a one-photon excitation peak at 500 nm will probably have a two-photon excitation maximum at <1,000 nm (Figure 3). Because two-photon excitation spectra are relatively broad, multiplex detection schemes in which two or more fluorophores are excited at a single wavelength and discriminated on the basis of different emission spectra are relatively easy to implement (some examples are included in Table 1). The two-photon absorption cross-section (σ) in units of GM (for Göppert-Mayer; 1 GM = 10^{-50} cm^4 seconds) quantifies the efficiency of TPE for different fluorophores and is plotted on the y-axis of excitation spectra (Figure 3). There are several published collections of two-photon excitation spectra and cross-sections that provide guidance on compatibility of dyes and probes with excitation sources.[21–25] Excitation wavelengths used in selected published TPE microscopy applications are listed in Table 1.

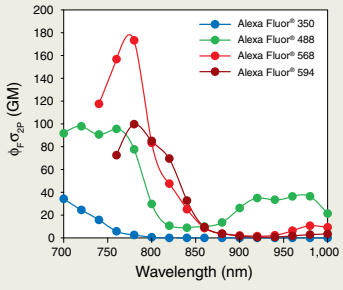

Figure 3—Two-photon excitation spectra of Alexa Fluor® 350, Alexa Fluor® 488, Alexa Fluor® 568, and Alexa Fluor® 594 dyes. The y-axis units are products of fluorescence quantum yields (Φ_F) and two-photon absorption cross-sections (σ). Data courtesy of Warren Zipfel, Cornell University.

Fluorophores and probes

TPE has added a new spectral dimension to fluorescence microscopy. Probes such as fura-2 (Ca^{2+}), SBFI (Na^+), monochlorobimane (glutathione), and DAPI (nuclear DNA), which were previously of limited utility in confocal microscopy due to their requirements for ultraviolet excitation, now have a new lease on life (Table 1). Furthermore, *in situ* imaging of small endogenous fluorophores such as serotonin and NADH that are almost inaccessible to one-photon excitation has now become practicable.[26] Organic fluorophores and fluorescent proteins typically have two-photon absorption cross-sections in the range 1–100 GM. However, fluorophores with smaller cross-sections (e.g., NADH, σ < 0.1 GM) can still generate sufficient TPE fluorescence for imaging purposes.[26] At the opposite extreme, Qdot® nanocrystals have cross-sections exceeding 10,000 GM, promising even further expansions to the utility of TPE imaging, particularly in the area of *in vivo* applications.[27,28] ■

References

1. Göppert-Mayer, M. (1931) *Ann Phys* 9:273–294.
2. Denk, W. et al. (1990) *Science* 248:73–76.
3. Girkin, J.M. and McConnell, G. (2005) *Micros Res Tech* 67:8–14.
4. Helmchen, F. and Denk, W. (2005) *Nat Methods* 2:932–940.
5. Squirrell, J.M. et al. (1999) *Nature Biotech* 17: 763–767.
6. Ruthazer, E.S. and Cline, H.T. (2002) *Real-Time Imaging* 8:175–188.
7. Eggeling, C. et al. (2005) *Chemphyschem* 6:791–804.
8. Hopt, A. and Neher, E. (2001) *Biophys J* 80:2029–2036.
9. Patterson, G. H. and Piston, D.W. (2000) *Biophys J* 78:2159–2162.
10. Dittrich, P.S. and Schwille, P. (2001) *Appl Phys B* 73:829–837.
11. Larson, D.R. et al. (2005) *J Cell Biol* 171:527–536.
12. Galbraith, J.A. and Terasaki, M. (2003) *Mol Biol Cell* 14:1808–1817.
13. Karotki, A. et al. (2006) *Photochem Photobiol* 82:443–452.
14. Brown, E.B. and Webb, W.W. (1998) *Methods Enzymol* 291:356–380.
15. Svoboda, K. and Yasuda, R. (2006) *Neuron* 50:823–839.
16. Diaspro, A. et al. (2005) *Q Rev Biophys* 38:97–166.
17. Rubart, M. (2004) *Circ Res* 95:1154–1166.
18. Zipfel, W.R. et al. (2003) *Nature Biotech* 21:1369–1377.
19. Helmchen, F. and Denk, W. (2005) *Nat Methods* 2:932–940.
20. Denk, W. et al. (2006) *Handbook of Biological Confocal Microscopy, Third Edition* (Pawley, J.B., Ed.), Springer, pp. 535–549.
21. Xu, C. et al. (1996) *Proc Natl Acad Sci U S A* 93:10763–10768.
22. Bestvater, F. et al. (2002) *J Microscopy* 208: 108–115.
23. Dickinson, M.E. et al. (2003) *J Biomed Opt* 8: 329–338.
24. Fisher, J.A. et al. (2005) *J Neurosci Methods* 148: 94–102.
25. Wokosin, D.L. et al. (2004) *Biophys J* 86:1726–1738.
26. Zipfel, W.R. et al. (2003) *Proc Natl Acad Sci U S A* 100:7075–7080.
27. Larson, D.R. et al. (2003) *Science* 300:1434–1436.
28. Michalet, X. et al. (2005) *Science* 307:538–544.